

## Optical Pseudogap from Iron States in Filled Skutterudites $A\text{Fe}_4\text{Sb}_{12}$ ( $A = \text{Yb}, \text{Ca}, \text{Ba}$ )

J. Sichelschmidt,<sup>1</sup> V. Voevodin,<sup>1</sup> H. J. Im,<sup>2,3</sup> S. Kimura,<sup>2,3</sup> H. Rosner,<sup>1</sup> A. Leithe-Jasper,<sup>1</sup> W. Schnelle,<sup>1</sup> U. Burkhardt,<sup>1</sup>  
J. A. Mydosh,<sup>4,1</sup> Yu. Grin,<sup>1</sup> and F. Steglich<sup>1</sup>

<sup>1</sup>Max Planck Institute for Chemical Physics of Solids, Nöthnitzer Straße 40, 01187 Dresden, Germany

<sup>2</sup>UVSOR Facility, Institute for Molecular Science, Okazaki 444-8585, Japan

<sup>3</sup>Department of Structural Molecular Science, The Graduate University for Advanced Studies, Okazaki 444-8585, Japan

<sup>4</sup>II. Physikalisches Institut, Universität zu Köln, 50937 Köln, Germany

(Received 21 July 2005; published 27 January 2006)

Optical investigations are presented of the filled skutterudites  $A\text{Fe}_4\text{Sb}_{12}$  with divalent cations  $A = \text{Yb}, \text{Ca}, \text{Ba}$ . For each of these compounds a very similar pseudogap structure in the optical conductivity develops in the far-infrared spectral region at temperatures below 90 K. Highly accurate local-density approximation electronic band structure calculations can consistently explain the origin of the pseudogap structure generated largely by transition metal  $3d$  states. In particular, a  $4f$ -conduction electron hybridization or strong correlations can be ruled out as origin for the pseudogap.

DOI: 10.1103/PhysRevLett.96.037406

PACS numbers: 78.30.-j, 71.20.Lp, 75.50.Bb

In recent years the concept of pseudogap formation has become a subject of prime importance for understanding strongly correlated electron systems and was successfully applied, e.g., to high- $T_c$  cuprates [1]. A particular interesting and nonclarified manifestation of charge gap formation is the pseudo or “hybridization” gap in nonoxide strongly correlated electron systems. The occurrence of such phenomena in several filled skutterudite compounds can be explained assuming  $4f$ -conduction electron hybridization [2] which in turn generates mass renormalized quasiparticles with a coherent Fermi liquid ground state. These quasiparticles influence thermodynamic quantities (“heavy-fermion” behavior) and cause the suppression of local magnetic moments at low temperatures. The energy scales of such hybridization effects are accessible, for instance, by probing the electron dynamics with optical spectroscopy [3]. At infrared frequencies as the temperature is reduced, a pseudogap can open in the optical conductivity because of coherent resonant scattering of conduction electrons on the hybridized charge carriers with enhanced electronic density of states (DOS) [4]. For the filled skutterudites such optical gap formations have been observed in  $\text{CeOs}_4\text{Sb}_{12}$  [5],  $\text{CeRu}_4\text{Sb}_{12}$ , and  $\text{YbFe}_4\text{Sb}_{12}$  [6]. However, caution is necessary when relating the pseudogaps to strong electron correlations. For example, the Heusler-type intermetallics  $\text{Fe}_2\text{VAl}$  and  $\text{Fe}_2\text{TiSn}$ , which have been proposed as  $d$ -electron heavy-fermion systems, display a pseudogap with a temperature independent magnitude. It implies a minor importance of strong correlations for the pseudogap formation which, moreover, was successfully explained by the electronic band structure [7,8]. This is in contrast to  $\text{FeSi}$  where the opening of a large gap ( $k_B \times 720$  K) is observed below 200 K. The latter is suggestive of a collective electronic behavior in  $\text{FeSi}$  due to strong  $d$ -electron correlations leading to a putative Kondo lattice picture [9].

The Fe-Sb skutterudites filled by nonmagnetic ions of alkali and alkaline-earth metals show remarkable properties which indicate the importance of magnetism originating in the polyanionic host [10]. In these compounds strong ferromagnetic spin fluctuations, a high DOS at the Fermi level  $E_F$  and, therefore, an enhanced electronic specific heat coefficient  $\gamma \approx 100\text{--}140$  mJ mol<sup>-1</sup> K<sup>-2</sup> are found [11,12]. Thus, with respect to these new findings the size of the contribution of the  $4f$ -conduction electron hybridization to the creation of an enhanced or heavy effective electronic mass in some rare-earth filled iron skutterudites becomes questionable. In  $\text{YbFe}_4\text{Sb}_{12}$  the Yb is nonmagnetic and stable divalent ( $4f^{14}$ ) as recently proven experimentally [12–14]. In contrast, previous optical investigations of  $\text{YbFe}_4\text{Sb}_{12}$  claim  $4f$ -related heavy-fermion properties reflected in a hybridization induced far-infrared (FIR) pseudogap [6]. In this Letter, we clarify the nature of this pseudogap by comparing the optical properties of  $\text{YbFe}_4\text{Sb}_{12}$  with those of  $(\text{Ca}/\text{Ba})\text{Fe}_4\text{Sb}_{12}$ . We will find the observed FIR pseudogap to reflect the fine details of the band structure near  $E_F$ , which can be understood in a single particle picture without including explicitly electron-electron correlations.

We have measured the optical reflectivity  $R(\omega)$  of  $A\text{Fe}_4\text{Sb}_{12}$  ( $A = \text{Yb}$  and  $\text{Ca}, \text{Ba}$ ) at a near-normal angle of incidence on well polished ( $0.3 \mu\text{m}$  grain) polycrystalline samples. They were prepared from blends of  $\text{FeSb}_2$ ,  $\text{Sb}$ ,  $\text{CaSb}_2$ , and  $\text{BaSb}_2$ , respectively [11].  $\text{YbFe}_4\text{Sb}_{12}$  was synthesized as described previously [12]. The powders were compacted by spark plasma sintering. Their structure, thermodynamic, transport, and magnetic properties were already reported [10–12]. A rapid-scan Fourier spectrometer of Michelson and Martin-Puplett type was used for energies  $\hbar\omega$  between 3 meV and 3 eV ( $2 \text{ K} < T < 300 \text{ K}$ ) and for higher energies at  $T = 300 \text{ K}$  only. Synchrotron radiation extended the energy range from 1.2 eV up to

30 eV [15]. For determination of  $R(\omega)$  the sample was coated *in situ* with gold and then used for measuring the reference spectrum.

To obtain accurate electronic structure information, a full-potential nonorthogonal local-orbital calculation scheme (FPLO) [16] within the local spin density approximation (LSDA) was utilized. In the fully relativistic calculations the exchange and correlation potential of Perdew and Wang [17] was used. As the basis set  $\text{Ca}(3s, 3p, 4s, 4p, 3d)$ ,  $\text{Ba}(5s, 5p, 6s, 6p, 5d)$ ,  $\text{Yb}(4f, 5s, 5p, 6s, 6p, 5d)$ ,  $\text{Fe}(3s, 3p, 4s, 4p, 3d)$ , and  $\text{Sb}(4s, 4p, 4d, 5s, 5p, 5d)$  states were employed. All lower lying states were treated as core states. The strongly correlated Yb 4*f* states were treated within the LDA + *U* scheme using an additional Coulomb repulsion of 8 eV [11,12]. To ensure accurate band structure and DOS, especially for flat bands, a very fine *k* mesh of 5551 points in the irreducible part of the Brillouin zone (125.000 in the full zone) was used.

The  $R(\omega)$  data are shown in Fig. 1 for  $T = 4$  and 300 K. The reflectivity above 0.5 eV (see inset) is determined by electronic interband transitions comparable to those observed in a variety of skutterudite compounds [5,6]. Below 0.5 eV typical metallic behavior is observed; i.e.,  $R(\omega)$  approaches unity towards zero energy and in the FIR region ( $<0.1$  eV)  $R(T)$  shows an increase with decreasing  $T$ . However, below  $T \approx 90$  K  $R(\omega)$  shows a pronounced suppression of up to  $\approx 4\%$  ( $T = 4$  K) with a minimum located at about the same energy (12 meV) for  $\text{CaFe}_4\text{Sb}_{12}$  and  $\text{YbFe}_4\text{Sb}_{12}$ , and at  $\approx 15$  meV for  $\text{BaFe}_4\text{Sb}_{12}$ . This suppression is not found in  $\text{AFe}_4\text{Sb}_{12}$  with the monovalent cations Na and K [18]. Using Kramers-Kronig relations,

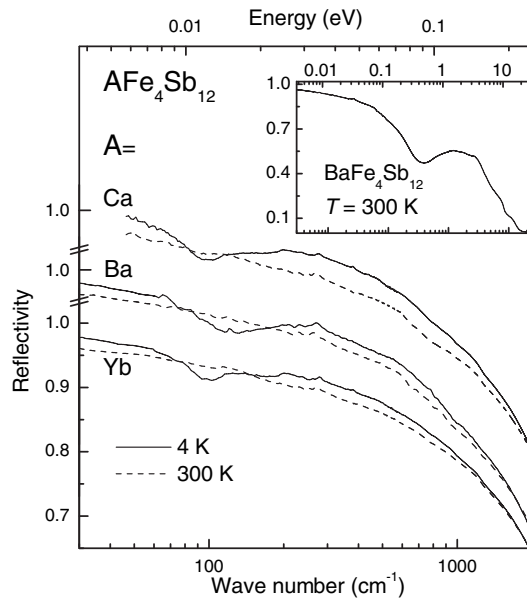


FIG. 1. Reflectivity spectra of  $\text{AFe}_4\text{Sb}_{12}$  ( $A = \text{Ca}, \text{Ba}, \text{Yb}$ ) at  $T = 4$  and 300 K. Inset shows the spectrum of  $\text{BaFe}_4\text{Sb}_{12}$  at  $T = 300$  K in the complete accessible spectral range.

we calculated the complex optical conductivity  $\sigma(\omega) = \sigma_1(\omega) + i\sigma_2(\omega)$  from  $R(\omega)$  [19]. Above energies of 30 eV, where an eventual small temperature dependence of  $R(\omega)$  has negligible influence on  $\sigma(\omega \approx 10$  meV), a free-electron approximation of the form  $R(\omega) \propto \omega^{-4}$  was used. We fitted the low-energy end  $\sigma(\omega \leq 30$  meV) to the electrical conductivity  $\sigma_{\text{dc}}(\omega \rightarrow 0)$  by a Drude-Lorentz function such that  $\sigma_{\text{dc}}$  values were described within  $\pm 20\%$ . Values  $\sigma_{\text{dc}}(T \rightarrow 0)$  of  $10 - 54 \times 10^3 \Omega^{-1} \text{cm}^{-1}$  were measured on the investigated samples [20]. Uncertainties of the  $\sigma(\omega)$  spectra due to variations of the low-energy extrapolation of  $R(\omega)$  are negligible for energies  $>6$  meV.

Figure 2 shows the dissipative part  $\sigma_1(\omega)$  of  $\sigma(\omega)$  at selected temperatures. In the FIR region, below  $\approx 50$  meV,  $\sigma_1(\omega)$  exhibits a pronounced  $T$ -dependent change. For all three compounds this feature is very similar regarding its energy position and absolute  $\sigma_1(\omega)$  value. At low  $T$ , the latter becomes partially suppressed between 3 and 17 meV, whereas it is enhanced with a broad shoulder between 17 and 60 meV, indicating the formation of a pseudogap in the optical charge excitations below  $\approx 17$  meV. For  $\text{BaFe}_4\text{Sb}_{12}$  the inset of Fig. 2 shows  $\sigma_1(T)$  at  $\hbar\omega = 10$  meV demonstrating the evolution of the pseudogap. The other compounds show a similar  $\sigma_1(T)$  behavior. Above  $T \approx 90$  K  $\sigma_1(T)$  shows conventional metallic behavior. Below  $T \approx 90$  K,  $\sigma_1(T)$  is continuously suppressed until at the lowest  $T$  it reaches a minimum value. As confirmed by our band structure cal-

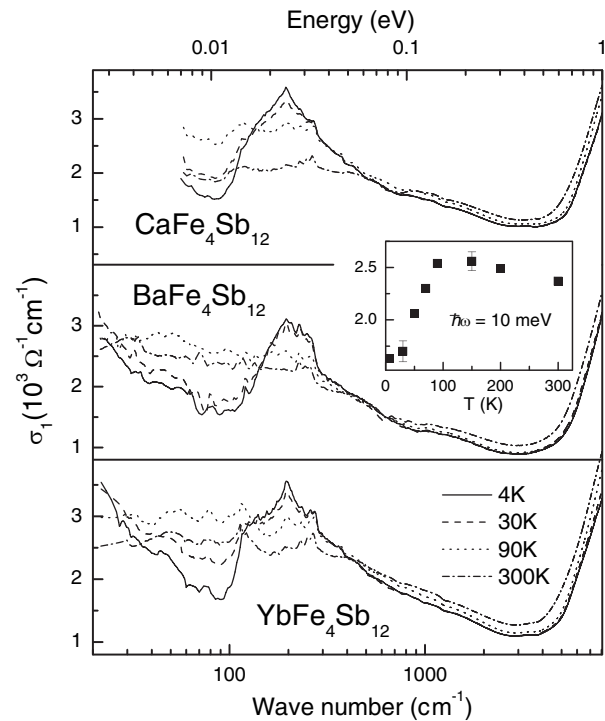


FIG. 2. Optical conductivity  $\sigma_1(\omega)$  of  $\text{AFe}_4\text{Sb}_{12}$  ( $A = \text{Ca}, \text{Ba}, \text{Yb}$ ) at  $T = 4, 30, 90, 300$  K. Inset shows  $\sigma_1(T)$  at  $\hbar\omega = 10$  meV for  $\text{BaFe}_4\text{Sb}_{12}$ .

culations (see below) this behavior indicates the gradual appearance of sharply energy separated DOS structures until their optimum resolution is approached at the lowest  $T$ .

The temperature of  $\approx 90$  K, above which the pseudogap is smeared out, roughly corresponds to the pseudogap energy of  $\approx 12$  meV where the minimum of  $\sigma_1(\omega)$  is found and which seems to be temperature independent. Therefore, when compared with FeSi [9],  $\sigma_1(T)$  of  $A\text{Fe}_4\text{Sb}_{12}$  is compatible with weak electronic correlations only. This is furthermore evidenced by an inspection of the optical spectral weight distribution with temperature within the energy region where the pseudogap evolves. By integrating  $\sigma(T)$  between 3 and 250 meV we found that the spectral weight is conserved within 5%. Thus, energy scales 1 order of magnitude larger than the gap energy are involved in the charge dynamics of  $A\text{Fe}_4\text{Sb}_{12}$ . Quite differently, for FeSi the charge dynamics involves high energy scales, much larger than the gap energy. There the spectral weight lost on gap formation at low  $T$  is spread over an energy range of order eV which is associated with strong electronic correlations [9].

In order to facilitate a comparison of the compound-dependent changes, Fig. 3(a) shows the ratio  $\sigma_1(4\text{ K})/\sigma_1(90\text{ K})$  which relates  $\sigma_1(\omega)$  with and without pseudogap. The plot clearly demonstrates the almost identical optical behavior of  $\text{CaFe}_4\text{Sb}_{12}$  and  $\text{YbFe}_4\text{Sb}_{12}$  even on a remarkably low-energy (meV) scale, which is consistent with the same valency of Yb and Ca in  $A\text{Fe}_4\text{Sb}_{12}$  [12]. For  $\text{BaFe}_4\text{Sb}_{12}$  the FIR electronic structure shows a shift of

$\approx 2.5$  meV which we attribute to an analogous change in the band structure, see below. The similarity of the optical properties of  $A\text{Fe}_4\text{Sb}_{12}$  indicates that the charge dynamics is mainly related to the electronic configuration of the  $\text{FeSb}_3$  host network, as expected from their similar bulk properties. Furthermore, the pseudogap appears at about the same temperature where  $\sigma_{\text{dc}}(T)$  shows a shoulder [6,20,21]. These observations are consistent with the purely itinerant magnetism of  $A\text{Fe}_4\text{Sb}_{12}$ . The FIR pseudogap may be interpreted as a direct low-temperature signature of the electronic band structure.

This relation of  $\sigma_1(\omega, T)$  to the band structure is corroborated by the presence of structures close to the pseudogap [Fig. 3(b)]. The phonon contributions to  $\sigma_1(\omega)$  were identified with the skutterudite  $\text{CoSb}_3$ , which is a narrow gap (118 meV) semiconductor [22], where phonon excitations in the FIR region are not suppressed by metallic screening. The structures in  $\sigma_1(\omega)$  of  $\text{CaFe}_4\text{Sb}_{12}$  and  $\text{BaFe}_4\text{Sb}_{12}$  between 30 and 35 meV, and close to 15 meV can be identified with infrared active optical phonons [Fig. 3(b)]. Other filled skutterudites show very similar phonon characteristics [6]. However, the sharp feature at 24 meV and a weak feature for  $\text{CaFe}_4\text{Sb}_{12}$  at 47 meV have no counterpart in  $\sigma_1(\omega)$  of  $\text{CoSb}_3$  and therefore do not originate from phonons. We attribute them to flat bands in a small  $k$ -space region causing narrow peaks in the DOS. This partly explains the large  $\gamma$  values whose enhancement also results from strong spin fluctuations reflecting a large Sommerfeld-Wilson (SW) ratio ( $R_{\text{SW}} \gg 1$ ) [23]. The Yb, Ca, Ba, and Sr filled compounds are nearly ferromagnetic metals [11,12,21] with  $R_{\text{SW}} \approx 24$  [12].

The calculated DOS, especially for  $\text{CaFe}_4\text{Sb}_{12}$  and  $\text{YbFe}_4\text{Sb}_{12}$  [12], but also for the Ba compound, are very

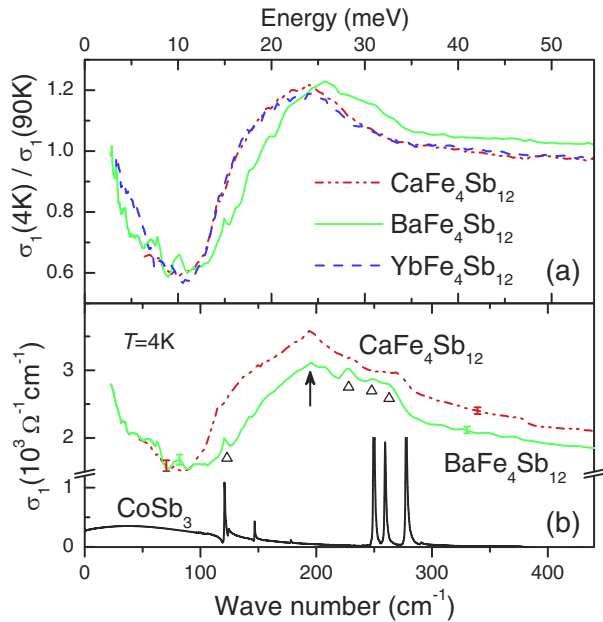


FIG. 3 (color online). (a) Optical conductivity  $\sigma_1(\omega, T = 4\text{ K})$  related to  $\sigma_1(\omega, T = 90\text{ K})$ . (b) Comparison of  $\sigma_1(\omega)$  of  $\text{CaFe}_4\text{Sb}_{12}$  and  $\text{BaFe}_4\text{Sb}_{12}$  with optical phonons in  $\text{CoSb}_3$ . Triangles indicate phonon structures in  $\sigma_1(\omega)$  of  $\text{CaFe}_4\text{Sb}_{12}$  and  $\text{BaFe}_4\text{Sb}_{12}$ . Arrow indicates a structure with no phonon counterpart.

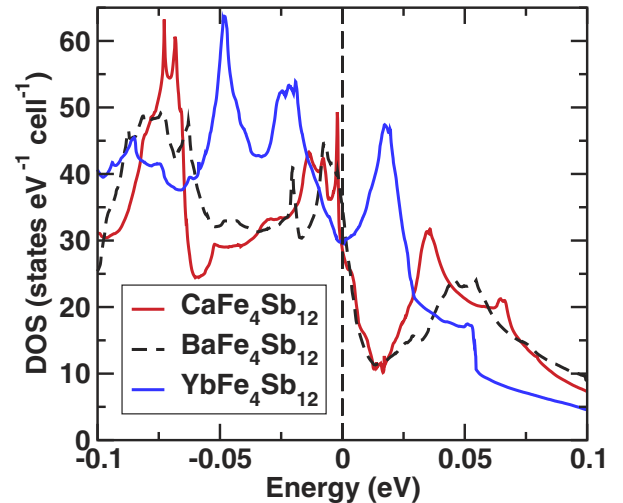


FIG. 4 (color online). Total DOS of  $A\text{Fe}_4\text{Sb}_{12}$  near the Fermi level. For  $A = \text{Yb}$  the scalar relativistic result is shown without spin orbit coupling (see text). For  $A = \text{Ca, Ba}$  the spin orbit coupling was included leading to an upward shift and broadening of the peak  $\approx 50$  meV above  $E_F$ .

similar for the entire valence region. The bottom of the valence band is built up by Sb-5*p*-Fe-3*d* hybrid states, whereas the region close to  $E_F$  is dominated by Fe-3*d* states with only a small admixture of Sb states [11]. The contribution of the cations to the valence band is negligible. For  $\text{YbFe}_4\text{Sb}_{12}$  a physically correct description of the strongly correlated 4*f* states requires the explicit treatment of the strong Coulomb repulsion, modeled here within the LDA +  $U$  scheme. At present, this scheme is implemented only scalar relativistically in the FPLO code. The resulting DOS is, even for details, basically identical with the scalar relativistic calculation for  $\text{CaFe}_4\text{Sb}_{12}$  [12]. In the latter case, the inclusion of the spin orbit coupling leads to an upward shift of the peak and a slight broadening. Because of the negligible contribution of the cations, identical changes can be expected for  $\text{YbFe}_4\text{Sb}_{12}$  upon inclusion of spin orbit coupling.

The pseudogap and its different appearances in  $\text{BaFe}_4\text{Sb}_{12}$  and  $\text{CaFe}_4\text{Sb}_{12}$  as well as the sharp features are well reproduced (Fig. 4). For all three compounds a pronounced minimum in the DOS is followed by a narrow peak at about 35 meV for Ca and 45 meV for Ba. The inclusion of spin orbit coupling shifts the pseudogap to about 15 meV higher energies. The narrow peak originates from a very flat band region around the  $\Gamma$  point. The peaks in the DOS are in good agreement with the optical data, even the correct tendency for the peak shift in the Ba compound [Fig. 3(a)] is observed.

We suggest two reasons for the small differences in the energy position of the DOS peaks compared to the optical data: (i) LSDA underestimates the influence of electronic correlations. Although the Fe 3*d* states generating the DOS peak close to  $E_F$  show itinerant behavior, a small renormalization of the band width and position can be expected from Hubbard-type corrections. (ii) The coupling to other degrees of freedom like phonons or spin fluctuations may lead to band renormalization shifts. Several bands with different orbital character cross the Fermi level. From the differing electron-phonon couplings in these bands, shifts of the Fe related bands versus the Sb related states can be expected. For large differences in these couplings, such shifts can be as large as 100 meV in  $\text{MgB}_2$  [24]. The strong spin fluctuations present in  $\text{AFe}_4\text{Sb}_{12}$  [11,12] can cause similar effects. In general, the very good agreement between the LSDA calculated electronic structure and the optical data suggests a minor relevance of Coulomb correlations in particular for describing the FIR optical pseudogap in  $\text{AFe}_4\text{Sb}_{12}$ .

We conclude that the almost identical optical pseudogap structure in  $\text{AFe}_4\text{Sb}_{12}$  with  $A = \text{Yb, Ca, Ba}$  is consistent with the results of high-resolution LSDA band structure calculations which indicate a pseudogap evolution in the electronic excitations by lowering the temperature. The

observation of sharp peaks in the optical conductivity agrees with the LSDA description and provides further evidence for band structure effects. Therefore, at least for  $\text{AFe}_4\text{Sb}_{12}$  with  $A = \text{Yb, Ca, Ba}$ , only weak electronic correlations within the Fe3*d*-Sb5*p* bands seem to be present. This is a completely different mechanism than the hybridization gap scenario for 4*f* heavy-fermion compounds leading, however, to similar optical spectra. Keeping in mind the relevance claimed for the hybridization gap picture in other filled skutterudites [5,6] our results, with unexpected clearness, demonstrate that FIR optical pseudogaps can originate from the single particle electronic band structure of these systems.

The work was partially supported by the joint studies program of the Institute for Molecular Science (IMS). J.S. acknowledges support from the international collaboration program of the IMS, Okazaki, H.R. from the Emmy-Noether-Program of the DFG, and J. A. M. from the Alexander von Humboldt Foundation.

- 
- [1] D.N. Basov and T. Timusk, Rev. Mod. Phys. **77**, 721 (2005).
  - [2] M.B. Maple *et al.*, Physica B (Amsterdam) **328**, 29 (2003).
  - [3] L. Degiorgi, Rev. Mod. Phys. **71**, 687 (1999).
  - [4] L. Degiorgi, F. Anders, and G. Grüner, Eur. Phys. J. B **19**, 167 (2001).
  - [5] M. Matsunami *et al.*, J. Phys. Soc. Jpn. **72**, 2722 (2003).
  - [6] S. V. Dordevic *et al.*, Phys. Rev. Lett. **86**, 684 (2001).
  - [7] H. Okamura *et al.*, Phys. Rev. Lett. **84**, 3674 (2000).
  - [8] S. V. Dordevic *et al.*, Phys. Rev. B **66**, 075122 (2002).
  - [9] Z. Schlesinger *et al.*, Phys. Rev. Lett. **71**, 1748 (1993).
  - [10] A. Leithe-Jasper *et al.*, Phys. Rev. Lett. **91**, 037208 (2003).
  - [11] A. Leithe-Jasper *et al.*, Phys. Rev. B **70**, 214418 (2004).
  - [12] W. Schnelle *et al.*, Phys. Rev. B **72**, 020402(R) (2005).
  - [13] D. Bérardan *et al.*, J. Alloys Compd. **351**, 18 (2003).
  - [14] D. Bérardan, E. Alleno, and C. Godart, J. Magn. Magn. Mater. **285**, 245 (2005).
  - [15] K. Fukui *et al.*, Nucl. Instrum. Methods Phys. Res., Sect. A **467-468**, 601 (2001).
  - [16] K. Koepf and H. Eschrig, Phys. Rev. B **59**, 1743 (1999).
  - [17] J.P. Perdew and Y. Wang, Phys. Rev. B **45**, 13 244 (1992).
  - [18] J. Sichelschmidt *et al.* (to be published).
  - [19] M. Dressel and G. Grüner, *Electrodynamics of Solids* (Cambridge University Press, Cambridge, England, 2002).
  - [20] W. Schnelle *et al.* (to be published).
  - [21] E. Matsuoka *et al.*, J. Phys. Soc. Jpn. **74**, 1382 (2005).
  - [22] K. Koga, K. Akai, K. Oshiro, and M. Matsuura, Phys. Rev. B **71**, 155119 (2005).
  - [23] H.-A. Krug von Nidda, R. Bulla, N. Büttgen, M. Heinrich, and A. Loidl, Eur. Phys. J. B **34**, 399 (2003).
  - [24] H. Rosner, J.M. An, W.E. Pickett, and S.-L. Drechsler, Phys. Rev. B **66**, 024521 (2002).